PAPER

LET dependent response of GafChromic films investigated with MeV ion beams

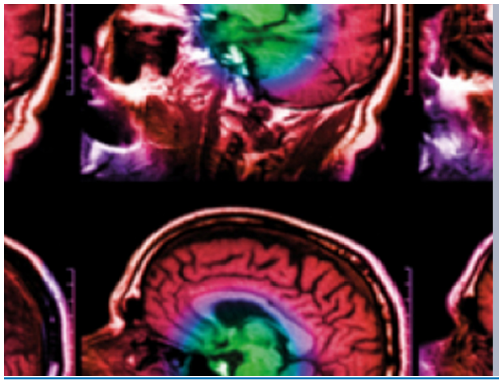

IOP Publishing Phys. Med. Biol. 63 (2018) 245021 (9pp) https://doi.org/10.1088/1361-6560/aaf34a

Physics in Medicine & Biology

IPEM Institute of Physics and Engineering in Medicine

RECEIVED
12 July 2018

REVISED
12 November 2018

ACCEPTED FOR PUBLICATION
23 November 2018

PUBLISHED
18 December 2018

PAPER

LET dependent response of GafChromic films investigated with MeV ion beams

V Grilj[1] and D J Brenner

Center for Radiological Research, Columbia University Irving Medical Center, New York, NY, United States of America

[1] Author to whom any correspondence should be addressed.

E-mail: vg2400@cumc.columbia.edu

Keywords: LET, signal quenching, under-response, unlaminated GafChromic films, EBT3, MD-V3, ions

Abstract

The change in optical properties of GafChromic films depends not only on the absorbed dose, but also on the linear energy transfer (LET) of the ionizing radiation. The influence of LET on the film dose-response relationship is especially important when films are applied for dosimetry of energetic charged particles. In the present study, we examined the response of the unlaminated EBT3 and MD-V3 films to proton, deuterium and helium beams with energies in the range of several megaelectronvolts (MeV). Films were exposed to doses up to 200 Gy and a model based on the bimolecular chemical reaction was chosen to fit the measured film signals. The LET in the active layers of the films and the dose correction factors were computed with Monte Carlo software TRIM. Signal quenching, observed for all ion beams in comparison to x-rays, was investigated as a function of the LET in the range of 10–100 keV μm^{-1}. The response of the films got weaker with increasing the LET and showed no dependence on the ion species. The LET effect was quantified by introducing a modified expression for the relative effectiveness (RE) by which a unique RE value is assigned to a single LET. The RE defined in that way decreased from about 90% for LET of 10 keV μm^{-1} to less than 50% for LET of 100 keV μm^{-1}. Similar behavior was observed for EBT3 and MD-V3 film models.

1. Introduction

The newest generation of GafChromic (Ashland ISP, Wayne, NJ) radiosensitive films represents current state of the art in film dosimetry (Devic 2011, Devic *et al* 2016, Das 2018). Advantages like tissue equivalence, no need for post-irradiation processing, low sensitivity to ambient light and simple readout with flatbed scanners triggered a widespread use of films for quality assurance (QA) measurements in external beam radiotherapy (Wen *et al* 2016, Steenbeke *et al* 2016) as well as brachytherapy (Palmer *et al* 2013). Because of a sub-millimeter resolution (Mirza *et al* 2016), GafChromic films are especially suitable for 2D and 3D dose profiling in procedures like photon or proton intensity modulated radiotherapy (IMRT) (Ju *et al* 2010, Iqbal *et al* 2018) or proton pencil-beam scanning (PBS) (Krzempek *et al* 2018). In such cases, commonly used arrays of ionization chambers with resolution of several millimeters do not provide adequate spatial precision.

It is a desirable property of any radio-dosimeter to be independent of the energy of the radiation quality being measured. Over the years of development, GafChromic films have been successfully optimized to reduce the energy dependence of their response to photons and electrons. For example, recent EBT3 model exhibits less than 5% variation in response to photons over an effective energy range of 50 keV–6 MeV (Massillon-JL *et al* 2012, Bekerat *et al* 2014). The same film model was found to have negligible dependence on electron beam energies ranging from 6 MeV to 16 MeV (Sipilä *et al* 2016). The situation is different for ultraviolet (UV) photons, where the darkening of the unlaminated EBT3 film was shown to be strongly dependent on the wavelength of the light in the 207–328 nm range (Welch *et al* 2017). When it comes to their performance with ion beams, GafChromic films show a significant dose under-response. It manifests as a weaker colorization of the film exposed to ions in comparison to x-rays or γ-rays, and was observed with all three external beam therapy (EBT) film models (EBT, EBT2, EBT3). For protons the under-response occurs at the Bragg peak region (Martišíková and Jäkel

2010, Perles *et al* 2013, Fiorini *et al* 2014, Reinhardt *et al* 2015, Vadrucci *et al* 2015, Battaglia *et al* 2016, Castriconi *et al* 2017), while for carbon ions it exists along the full dose deposition curve (Martišíková and Jäkel 2010, Castriconi *et al* 2017). In both cases, the effect was attributed to the enhancement of the linear energy transfer (LET) by either the decrease in the ion's energy as they slow down in the material (protons) or the increase in the ion's mass (carbon ions).

Two mechanisms were proposed to account for the observed signal quenching (Kirby *et al* 2010). The first was that a significant portion of densely spaced free radicals introduced by high LET radiation have a chance to recombine without initiating the polymerization of colorless diacetylene monomers (lithium salt of pentacosa-10,12-dyionic acid, LiPCDA) which are the common active component in GafChromic films. Since the coloration of the film occurs as a consequence of the polymerization process, fewer polymerization events will result in a loss of signal. The alternate explanation relies on the interplay between the density of ionization sites and the microcrystalline structure of the film active layer. Diacetylene monomers are packed in rod-like crystals whose size depends on the particular film model (2 μm $\times$ 15 μm for EBT3 (Schoenfeld *et al* 2014)). Inside the crystal lattice, polymerization sites (monomers) are spaced with some definite separation. For a high LET ion all sites near a single particle track get ionized and the film response saturates, leaving a portion of the particle's energy 'wasted' without contributing to film darkening.

The purpose of this work is to study the LET dependence of GafChromic films with different ion beams having energies of several megaelectronvolts (MeV). Such beams are regularly used in radiobiological experiments including cells, tissues and small animals (Marino 2017). Because of their short range in material, MeV ions require the use of the unlaminated film versions with active layers presented at the surface of the film. Also, high LET values (above several keV μm^{-1}) characteristic for MeV ions are expected to result in a pronounced signal quenching, making accurate dose estimation challenging. To address these issues, we exposed two unlaminated film models, EBT3 and MD-V3, to several monoenergetic ion beams achieving almost uniform LETs in the active layers of the films. Afterwards, we applied the bimolecular model proposed by Perles *et al* (2013) to fit the data and quantified the LET dependence by introducing a modified definition of the film relative effectiveness. To our knowledge, this is the first time that the LET effect in radiosensitive films was investigated with the 'quasi' mono-LET beams spanning a broad LET range of 10–100 keV μm^{-1}.

2. Materials and methods

2.1. Unlaminated GafChromic films

The majority of GafChromic film models comprise an active layer sandwiched between two polyester laminates (Devic *et al* 2016). Unfortunately, that structure is not compatible for use with MeV ions whose ranges are often shorter than or comparable with the thickness of the polyester layer. Instead, the viable option is to use the so-called 'unlaminated' films. Their layout differs from the standard one by lacking the polyester laminate on one side of the active layer, making it easier for the low energy ions to interact with the active layer and induce the signal. Unlaminated versions of two film models, EBT3 and MD-V3, were obtained from the film manufacturer. The diagrams of film structures are given in figure 1 and the atomic compositions of the corresponding active layers are given in table 1. Both films feature a 125 μm thick polyester base, which is coated with an active layer. The thickness of the active layer is 14 μm for unlaminated EBT3 and 12 μm for unlaminated MD-V3 film, as provided by the manufacturer. A single batch of each film was used in this study (EBT3 lot 02171601 and MD-V3 lot 11201503).

2.2. Film irradiations

The 20.3 cm $\times$ 25.4 cm sheets of unlaminated EBT3 film and 12.7 cm $\times$ 12.7 cm sheets of unlaminated MD-V3 film were cut into approximately 1.27 cm $\times$ 2.54 cm pieces and irradiated in air with ions and x-rays. Eight different ion/energy combinations were used to vary the average LET in the active layer of the film from 10 keV μm^{-1} to 100 keV μm^{-1}. X-rays were used for comparison as a low LET radiation. Dose responses of the films were evaluated in the dose range from 0 Gy to 200 Gy for all radiation qualities except for x-rays where maximum applied dose was 128 Gy. Films were stored post irradiations in light tight box at room temperature for 72 h before scanning. In this way the effect of long term development was minimized (Devic *et al* 2016).

2.2.1. Ion beam irradiations

The 5.5 MV Singletron accelerator was used to produce proton, deuterium and helium ion beams of various energies (Marino 2017) (see table 2). Particular combinations of ion species and energies were chosen with the goal of covering a wide range of LETs while keeping the change of LET throughout the active layers under 20% of its' mean value. Irradiations were performed at the Radiological Research Accelerator Facility (RARAF) track segment facility where a vertical beam of accelerated ions propagates through a set of apertures for defining the beam size and monitoring the beam current. Ion beam exits into the atmosphere through 6 mm $\times$ 20 mm

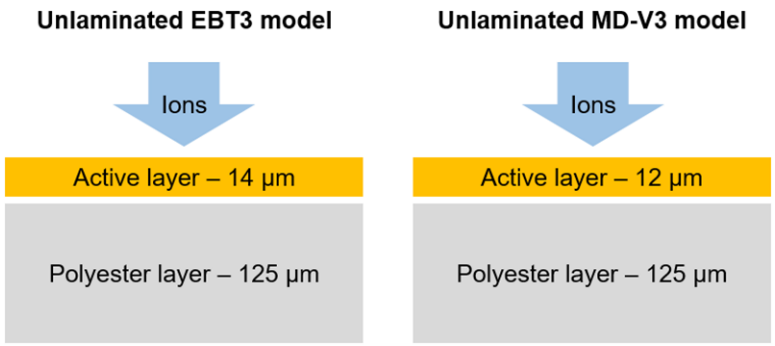

Figure 1. Diagram of the unlaminated film structure. Ion beam irradiations were done with the active layer facing the beam.

Table 1. Density and chemical composition of the active layers of the unlaminated films used.

		Active layer composition by atomic%								
Film model	Density/g cm^{-3}	H	Li	C	N	O	S	Na	Cl	Al
EBT3	1.35	55.8	0.6	31.1	0.4	10.5	0.1	0.1	0.1	0.1
MD-V3	1.25	57.8	0.5	27.8	1.5	12.3		0.1	0.1	

Table 2. Energies, average LETs and dose correction factors of proton (H^+), deuterium (D^+) and helium (He^{2+}) beams used in this work. Percentages in the parenthesis in LET columns show the relative change in LET throughout the active layers of unlaminated EBT3 and MD-V3 films.

		EBT3		MD-V3	
Ion	Energy	LET	Corr. factor	LET	Corr. factor
H^+	4.5	12 (4%)	0.98	12 (4%)	1.00
H^+	3.4	16 (6%)	1.00	15 (6%)	1.02
H^+	2.7	20 (10%)	0.99	19 (8%)	1.01
D^+	4.5	22 (6%)	1.00	21 (4%)	1.03
D^+	3.5	28 (10%)	1.00	26 (8%)	1.02
D^+	2.5	40 (18%)	0.96	37 (16%)	0.96
He^{2+}	11	80 (8%)	1.02	75 (6%)	1.05
He^{2+}	9	99 (16%)	1.02	93 (12%)	1.04

exit aperture which is covered by 2.9 μm thick havar foil. The beam was defocused with the use of two magnetic quadrupoles so that the variation in beam intensity was less than 5% across the exit aperture. Beam uniformity was checked by moving a solid state detector to eight different positions along the length of the exit aperture and counting the number of particles coming out at each position. Pieces of EBT3 and MD-V3 films were placed in sample dishes that are composed of a 6 μm thick mylar foil suspended over the metal ring (2″ diameter). Films were oriented so that the active layer was looking downwards and touching the mylar foil. A flat irradiation wheel with a capacity for 20 sample dishes was remotely rotated by a stepping motor to scan dishes with films over the beam. There was a 5.8 mm air gap between the vacuum window and the bottom of the dish. Irradiations were done in the following sequence. The beam current was constantly monitored by integrating the current from one of the apertures (also called the beam monitor) that wipes off a small portion of the beam penumbra. The beam monitor controls the rate at which the irradiation wheel moves and consequently the dose that is delivered to the samples. In particular, the wheel waits at each position until the appropriate number of counts is acquired by the beam monitor, then rotates by one step and waits again for the same signal. The number of monitor counts per step required to deliver a desired dose was calibrated by performing a dosimetry protocol before the irradiations. The dosimetry protocol was run by the computer and consisted of scanning a custom made ionization chamber (mounted on a wheel identical to the irradiation wheel) and measuring the total dose deposited inside the chamber. In that way, the ionization chamber, which is of the parallel-plate type, filled with methane based tissue equivalent (TE) gas and operated in a current mode, mimics the trajectory of a sample dish. Moreover, the bottom part of the ionization chamber through which ions enter the collecting volume is identical to a sample dish, i.e. it is composed of a 6 μm thick mylar foil with the difference that the foil is in this case covered by a thin layer of carbon on the inner surface to provide electrical conduction. While the chamber is scanned over the beam, its' current output is integrated to give a total charge produced inside the collecting volume which

is a measure of the dose deposited to the tissue equivalent gas in the chamber. The initial rate of the rotation of the wheel with the chamber was predefined in the software. After the initial scan, a new number of counts per step was calculated based on the correction factor which is equal to a ratio between the desired dose and the dose that was actually deposited in the ionization chamber. The procedure was repeated until the correction factor becomes by less than 0.1% different from 1. At that point the dosimetry protocol was finished and the number of monitor counts per step that was last used was transferred to the irradiation protocol. An irradiation protocol was created by inputting a set of desired doses to the computer. The computer was then controlling the movement of the samples (films) over the beam at a rate that was determined previously by the dosimetry protocol. Dose rates for irradiations were around 0.2 Gy s^{-1} for all ion species. It is worth pointing out that within the described irradiation protocol films were exposed to doses that represent absorbed doses to the TE gas in the ionization chamber. The actual doses absorbed in the film active layers were calculated offline. More details about the dosimetry procedures and schematics of the track segment experiment can be found in papers by Bird *et al* (1980) and by Colvett and Rohrig (1979).

2.2.2. X-ray irradiations

X-ray irradiations were done with a Westinghouse Coronado orthovoltage x-ray machine operating at 250 kVp and 15 mA of electron current with a 0.5 mm Cu + 1 mm Al filter. The half value layer of our x-ray unit with the listed additional filters was measured to be 2 mm of Cu. The dose rate at the film location was 2 Gy min^{-1}. Dosimetry was done with a Victoreen model 570 condenser *R* meter and a 250r chamber. Although this is not the optimal ionization chamber for measuring the output of the x-ray unit, this detector was cross calibrated against film and TLDs measurements performed by an independent lab.

2.3. Film analysis

An Epson Perfection V700 Photo (Epson, Suwa, NGN, Japan) flat-bed scanner in transmission mode was used to digitize irradiated films as 48 bit RGB images in tagged image file format (TIFF). Before scanning the films, three preview scans were taken to warm up the scanner. It was noticed that taking up to five preview scans does not introduce any additional change in the colorization of the film. Films were scanned in sets with the resolution of 300 dpi. One set consisted of landscape oriented, vertically aligned pieces of either EBT3 or MD-V3 films that were exposed to the full range of doses of the same radiation quality. A matching unexposed piece of film that went through the same handling procedures as irradiated films was included with each set. No image correction due to the lateral scanner artifact (Lewis and Chan 2014) was required because films were placed along the middle line of the scan window forming only an inch-wide column.

Optical density (OD) measurements were done with image analysis program ImageJ (National Institute of Health, Bethesda, MD, USA). Raw pixel values (*PV*) from the red color channel were sampled from the 1 × 1 cm region of interest (ROI) placed over the central area of irradiated piece of film. Darkening of the film in the red channel was quantified in terms of the net optical density change, *netOD*, according to the following expression:

$$netOD = -\log\left(\frac{\overline{PV} - \overline{PV}_{dark}}{\overline{PV}_0 - \overline{PV}_{dark}}\right), \quad (1)$$

where $\overline{PV}$ and $\overline{PV}_0$ are the mean pixel values of exposed and unexposed films, respectively, averaged over the selected ROIs. $\overline{PV}_{dark}$ is the background scanner reading taken with a dark cardboard placed over the scan window. The corresponding uncertainty, σ_{netOD} was calculated by propagating the errors $\sigma_{\overline{PV}}$, $\sigma_{\overline{PV}_0}$ and $\sigma_{\overline{PV}_{dark}}$ which stand for standard deviations of the pixel values within the ROI. An additional 1% error was added to all σ_{netOD} values to account for the film and scanner reproducibility and film uniformity (León Marroquin *et al* 2016).

2.4. Monte Carlo simulations

The Monte Carlo simulation program TRIM (Ziegler *et al* 2008) was used to estimate the average LET of the projectile ions inside the active layers of films and inside the TE gas that fills up the ionization chamber that was used for dosimetry. All layers of materials that ions encounter on their way from the vacuum system to the target (film or ion chamber) were simulated with the program. Those include the 2.9 μm thick havar foil, 5.8 mm of the air gap and the 6 μm thick mylar foil that makes the bottom of the sample dishes and the ionization chamber. Atomic compositions and mass densities of materials were taken either from the data provided by the manufacturer (EBT3 and MD-V3 active layers and TE gas) or from the TRIM database (havar, mylar, air). Propagation of 100 000 ions was followed for each ion/energy/target combination. Average energy of ions was determined at the entrance and at the exit of the target layer of interest: 14 μm and 12 μm thick active layers of EBT3 and MD-V3 films, and 3.12 mm thick layer of methane based TE gas. Average LET was then calculated as the ratio between the energy deposited inside the layer and the thickness of the layer.

2.5. Dose calculations

Doses delivered to films during track segment irradiations were determined from the reading of the ionization chamber. To compare the film dose-responses to different ion beams we had to calculate the actual doses absorbed by the active layers of the exposed films. In case of charged particles, the dose absorbed by any material can be expressed with the use of the average LET as:

$$D = \frac{\overline{LET} \times \Phi}{\rho}, \tag{2}$$

where Φ stands for the fluence of particles and ρ stands for the mass density of the material. Equation (2) holds for the active layer of GafChromic film as well as for the TE gas in the ionization chamber. With Φ being equal in both cases, a simple relationship can be established between the dose absorbed by the chamber ($D_{chamber}$) and the dose absorbed by the film (D_{film}):

$$D_{film} = D_{chamber} \times \frac{\overline{LET}_{film}}{\overline{LET}_{TE\,gas}} \times \frac{\rho_{TE\,gas}}{\rho_{film}}. \tag{3}$$

The last two multiplication terms in equation (3) together form the dose correction factor. The average LET values obtained from TRIM simulations were used to compute the dose correction factors for ion beams used.

2.6. Dose-response relationship of GafChromic films

The dose-response relationship, i.e. the dependence of the *netOD* on the absorbed dose, is most commonly fitted with rational or 2nd order polynomial functions (Devic *et al* 2016, Das 2018). However, such functional forms are purely phenomenological, making it hard to correlate their parameters with the properties of the ionizing radiation. To be able to access the influence of the LET on the film response, we adopted the approach of Perles *et al* (2013) By following the reasoning that Candler (1960, 1962) applied on silver halide photographic films, they modeled the polymerization of diacetylene monomers in EBT2 film as a bimolecular nuclear reaction. Within the bimolecular model, the *netOD* is related to the dose by the following expression:

$$\frac{netOD}{netOD_{max} - netOD} = \left(\frac{D}{D_{1/2}}\right)^{p}, \tag{4}$$

where $netOD_{max}$ is the saturated value of *netOD* obtained with the same readout device when dose approaches infinity; D is the dose absorbed by the film; $D_{1/2}$ is the dose which results with $netOD = {}^{1}\!/_{2}\ netOD_{max}$; and p is a dimensionless constant known as the reaction order (Hitchcock and Robinson 1923). From the definition of the parameters in equation (4) it follows that $netOD_{max}$ is a property of the particular film batch and film reader used and p is the property of the nuclear reaction involved in the underlying polymerization process. Hence, only one parameter, $D_{1/2}$, can be accountable for the LET dependence of the film response.

The final expression that was used to fit the measured dose–response data was obtained by rearranging the equation (4) into:

$$netOD = netOD_{max} \frac{D^{p}}{{D_{1/2}}^{p} + D^{p}}. \tag{5}$$

The number of fitting parameters in equation (5) can be further reduced if $netOD_{max}$ is determined experimentally. To do so, we cut one piece from every film sheet that was used in the study and exposed it to the absorbed dose of 100 kGy delivered by 4.5 MeV protons, high enough to saturate both film types. Saturated films were processed and analyzed in the same way as described earlier. The variation in saturated signal among different sheets from the same batch was less than 3%. Therefore, we determined a single $netOD_{max}$ value for each film type (EBT3 and MD-V3) by averaging saturated *netOD* values from all film pieces of that type.

Matlab program (ver. R2017a) was used to do the non-linear fit of the equation(5) to the dose-response data. The least squares method was implemented to optimize the fitting parameters. Dose-response relationships of EBT3 film for all ion beams and x-rays were fitted at the same time with one global (shared) parameter and one local (independent) parameter. The same procedure was repeated for data sets measured with MD-V3 film. In both cases, the fitting parameters were defined as follows: parameter $netOD_{max}$ was fixed to be equal to the measured saturation value of *netOD*; parameter p was defined as a global parameter that has the same value for all dose-responses that belong to one film type (EBT3 or MD-V3), regardless of the LET; parameter $D_{1/2}$ was defined as the only local parameter that can change among the dose-responses measured with one film for different radiation qualities (different LETs). The $D_{1/2}$ parameter carries the LET dependence.

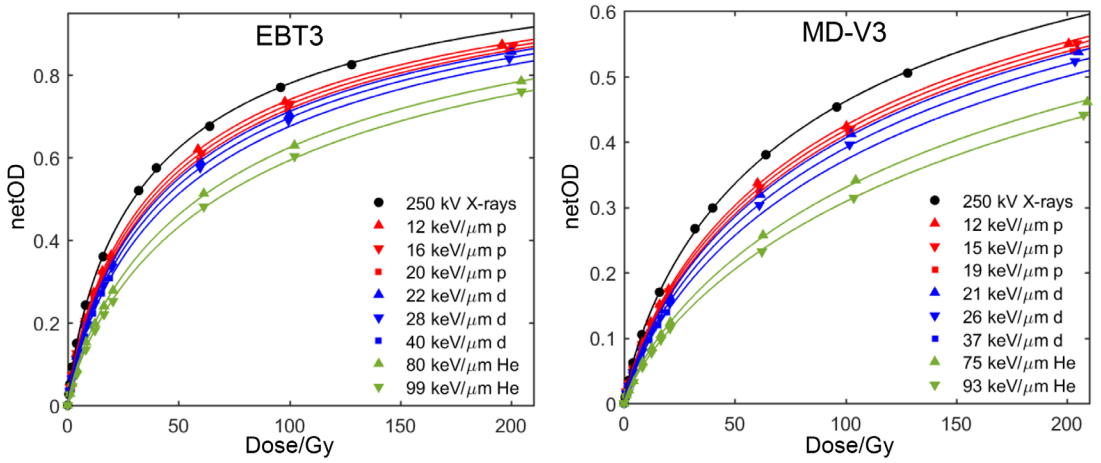

Figure 2. Darkening of the unlaminated EBT3 (left) and MD-V3 (right) films as a function of the dose of proton (p), deuterium (d) and helium (He) beams applied to the active layer of the film. The dose-response relationship for x-rays is shown for comparison. Solid lines present the fit of the bimolecular model to the data. All doses were determined with errors less than 5%. Errors in *netOD* are less than 3% for $netOD > 0.1$ and less than 6% for $netOD < 0.1$.

3. Results and discussion

3.1. Dose correction factors and LETs

Table 2 contains the LET values and the dose correction factors obtained from Monte Carlo simulations. The relative standard deviations for the calculated LET values (not shown in the table) were under 5%. The numbers in the parenthesis indicate the relative changes in LET throughout the active layer. They were calculated as the ratio of the difference between LET at the entrance and at the exit of the active layer and the mean LET value in that layer. The relative change in LET was under 10% for all beams except for the least energetic deuterium and helium beams where it was still lower than 20%. Therefore, we consider the ion beams used in this study to be 'quasi' mono-LET beams. The dose correction factors were computed in accordance to the equation (2). They were applied as multiplication factors to convert the doses measured by the ionization chamber into the actual doses delivered to the film active layers.

3.2. Film response to different LETs

Dose-responses of EBT3 and MD-V3 films exposed to proton, deuterium and helium ion beams and x-rays are shown in figure 2. The error bars are left out from the plots because of the large number of closely spaced data points. Doses applied by ion beams were estimated with relative standard deviations lower than 5% for the whole dose range. This was determined by including the uncertainties in dosimetry protocol and the calculated dose correction factors. The overall uncertainty in delivered x-ray doses was estimated to 5% at one standard deviation. The relative standard deviations of *netOD* values were less than 3% for $netOD > 0.1$ and up to 6% for $netOD < 0.1$. They were calculated by propagating the uncertainties defined in the *Film analysis* section and were similar in amounts among different radiation qualities.

Data in figure 2 show that an under-response occurs for all ion beams in comparison to the x-rays. Despite having different sensitivities, both film models display the quenching effect that becomes more pronounced the higher the LET is. Hence, a special attention should be paid to the use of GafChromic films for ion dosimetry. The optical response of the film will be affected not only by the dose, but also by the LET of the particle. It is also worth noticing that almost the same dose-response relationships were obtained for proton and deuterium beams with similar LETs. This indicates that the film response does not depend on the ion species itself.

3.3. Modelling of the dose-response relationships

Solid lines in figure 2 represent the fit of the bimolecular model to the dose-response data. The optimal fit parameters are summarized in table 3. Experimentally determined $netOD_{max}$ values are equal to 1.16 ± 0.03 and 0.91 ± 0.03 for EBT3 and MD-V3 films, respectively. For both film models, the fitted curves are in a good agreement with measurements over the full dose range that was investigated. The validity of the bimolecular model is best reflected in the fact that the accurate fits were achieved by fitting the dose-responses for all ion beams and x-rays at the same time with just two parameters, one that was shared among all data sets and only one that was independently varied for each data set. For comparison, we fitted the same data with the rational functional form that follows from equation (5) for $p = 1$. In this case, the fit started to deviate from the measurements at doses above 20 Gy and 60 Gy for EBT3 and MD-V3, respectively.

Table 3. Parameters p and $D_{1/2}$ that correspond to fitted curves shown in figure 2. $D_{1/2}$ values with standard deviations shown in parenthesis are listed as a function of the average LET expressed in keV/μm.

Model: $netOD = netOD_{max}\frac{D^p}{D_{1/2}{}^p + D^p}$			
EBT3		MD-V3	
$netOD_{max} = 1.16$[a]		$netOD_{max} = 0.91$[a]	
$p = 0.820 \pm 0.001$		$p = 0.820 \pm 0.001$	
LET	$D_{1/2}$/Gy	LET	$D_{1/2}$/Gy
X-rays	43.7 (0.2)	X-rays	98.4 (0.3)
12	50.1 (0.3)	12	117.4 (0.4)
16	52.7 (0.3)	15	122.3 (0.5)
20	55.3 (0.3)	19	127.4 (0.5)
22	56.9 (0.3)	21	130.6 (0.5)
28	60.9 (0.3)	26	141.7 (0.6)
40	66.7 (0.5)	37	157 (1)
78	83.0 (0.5)	73	199.3 (0.8)
96	94.6 (0.5)	90	226 (1)

[a] The values of $netOD_{max}$ were determined experimentally.

The same p value of 0.82 was obtained for EBT3 and MD-V3 films. It exactly matches the value reported by Perles *et al* (2013) for EBT2 film, implying that there is no difference in the dynamic of the nuclear reaction involved with the polymerization process in all three films. This result agrees with the similarity in the atomic composition of their active layers.

3.4. Relative effectiveness and the LET effect

Several authors (Martišíková and Jäkel 2010, Reinhardt *et al* 2015, Castriconi *et al* 2017) have tried to quantify the LET related signal quenching by introducing the concept of relative effectiveness (RE) expressed as the ratio between doses of photons (D_γ) and high LET radiation (D_{LET}) that induce equal film response ($netOD$):

$$RE = \left.\frac{D_\gamma}{D_{LET}}\right|_{netOD}. \tag{6}$$

However, because of the nonlinear dose-response relationship characteristic of GafChromic films, RE will take different values if calculated for different magnitudes of the film signal ($netOD$). Consequently, that equation (6) cannot provide a unique RE value that would depend on LET only.

The bimolecular model incorporates the LET dependence through parameter $D_{1/2}$. The values of $D_{1/2}$ that correspond to fitted ion beam dose-response relationships (table 3) are plotted against the average LET in figure 3. For comparison, the x-rays $D_{1/2}$ values are plotted with an average LET of 2 keV μm^{-1} that is usually attributed to 250 kVp photons [33]. Within the investigated LET range (10–100 keV μm^{-1}), the following linear fit adequately accounts for the change of $D_{1/2}$ with LET:

$$D_{1/2}(LET) = a * LET + D_{1/2}(0), \tag{7}$$

where a is the slope and $D_{1/2}(0)$ the intercept of the linear model. A number zero in the parenthesis in $D_{1/2}(0)$ refers to the infinitesimally small LET value. The fitted lines and the corresponding line equations are shown in figure 3. It can be noticed that $D_{1/2}$ values of x-rays lay within the 95% confidence intervals of the linear fits extrapolated down to low LETs. It follows that the relationship between $D_{1/2}$ and LET does not deviate significantly from the linear trend even below 10 keV μm^{-1}. The intercepts $D_{1/2}(0)$ of 45 Gy for EBT3 and 103 Gy for MD-V3 can be then considered as the lowest doses (delivered by radiation characterized by the infinitesimally small LET) required to induce the signal equal to one half of the saturation level. The difference between $D_{1/2}(LET)$ and $D_{1/2}(0)$ represents the 'wasted' dose which linearly increases with LET. It is worth now to consider again the two possible explanations of the LET effect described in the Introduction. If the main mechanism that accounts for the signal quenching is the recombination of the densely produced free radicals, then we would expect the 'wasted' energy to rise with higher powers of LET. The reason is that recombination includes more than one substance and its rate is usually proportional to the concentrations of the recombining substances. In our case, those concentrations are linearly proportional to LET (ionization density) so it turns out that the amount of the recombined radicals, and therefore the amount of 'wasted' energy, should roughly rise with LET squared, or even higher exponents if more than two substances recombine. Conversely, we hypothesize that the observed linearity favors the other proposed explanation that assumes the interplay between LET and the spacing of the

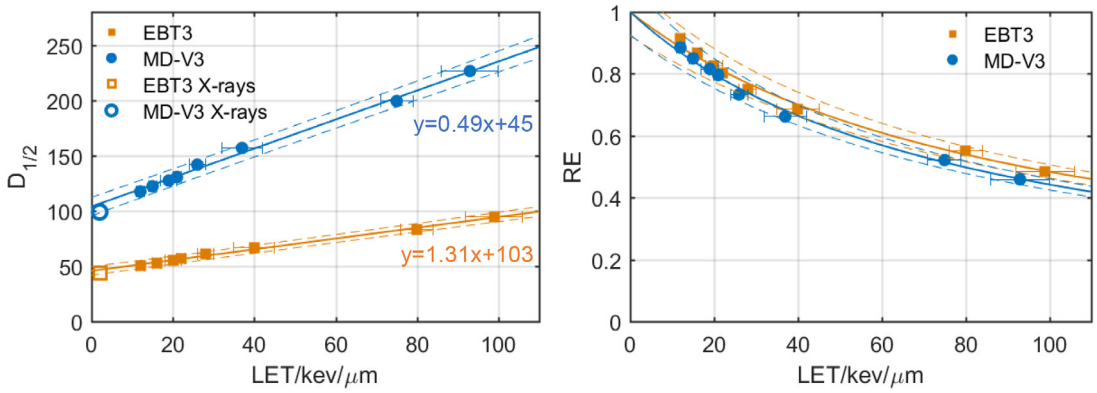

Figure 3. $D_{1/2}$ (left) and relative effectiveness (right) as a function of the average LET in the film active layer. The open symbols near the *y*-axis on the left graph represent the $D_{1/2}$ values for x-rays. The uncertainty bars corresponds to one standard deviation of the mean. Vertical error bars are smaller than the symbol size. Intermittent lines represent the bounds of the 95% confidence interval.

polymerization sites. The ionizations produced in space with no polymerization sites contribute to the 'wasted' energy. Any increase in ionization density (LET) results then with proportionally higher amount of energy that is not spent in polymerization of the LiPCDA monomers.

Additionally, in this work we suggest a modified expression for the relative effectiveness, which includes the ratio between $D_{1/2}(0)$ and $D_{1/2}$ associated with a particular LET:

$$RE = \frac{D_{1/2}(0)}{D_{1/2}(LET)}. \tag{8}$$

RE defined in that way is a function of LET only and has no dependence on the film signal which makes it suitable for comparing film responses to radiation qualities having different LETs. Nevertheless, determining $D_{1/2}(0)$ is an extensive procedure because in order to obtain enough $D_{1/2}(LET)$ values to apply a linear fit it requires measurements of dose-response relationships for a number of beams having different LETs. Alternatively, $D_{1/2}(0)$ can be replaced by $D_{1/2}$ of any low LET radiation like x-rays or γ-rays. In that way only two dose-response relationships have to be measured. We applied the equation (8) to calculate the relative effectiveness of EBT3 and MD-V3 films for the ion beams used. The results are shown in figure 3 as a function of the LET. The rate by which RE decreases with LET is slightly higher for MD-V3 than for EBT3. It might be the indication of the larger spacing between the dyacetilene monomers that makes MD-V3 a bit more sensitive to signal quenching caused by the energy deposited away from the polymerization sites. However, in both cases RE drops quite fast, starting from around 90% for 10 keV μm^{-1} and reaching almost 50% for 80 keV μm^{-1}. Similar LET levels are commonly achieved at the spread-out Bragg peak (SOBP) regions of proton and carbon therapy beams. Knowing then how the film response depends on LET, is of the utmost importance if significant errors in dose estimation are to be avoided.

4. Conclusions

We demonstrated the compatibility of the unlaminated GafChromic films for dosimetry of short range MeV ion beams. Unlaminated films can complement or be an alternative to the conventional dosimeters used in radiobiological accelerator facilities. In general, one of the main issues with film dosimetry of energetic ion beams is the LET related quenching of the signal. We investigated the LET effect for two unlaminated film models, EBT3 and MD-V3. Both films displayed a decrease in response if the dose was applied by ions having higher LET.

The bimolecular model provided accurate fit of the dose-response relationships for all ion beams and x-rays. The model easily accounted for the LET effect by having one of the parameters depending on the LET. We showed that the dose that does not contribute to the signal, the so called 'wasted' dose, increases linearly with LET. This result supported the explanation by which the finite spacing between polymerization sites is responsible for the observed LET dependence. Additionally, we proposed a way to define the relative effectiveness of the film so that it can be used to uniquely quantify the relationship between the film under-response and LET.

Acknowledgments

This work is supported by Grant number P41 EB002033 to The Radiological Research Accelerator Facility from the National Institute of Biomedical Imaging and Bioengineering. We are grateful to Ashland ISP for providing the unlaminated version of the MD-V3 film model which is not commercially available yet. The authors would

also like to thank David Welch from RARAF for instructions on the film analysis procedure and for the useful comments regarding the work presented in this paper.

ORCID iDs

V Grilj https://orcid.org/0000-0001-6573-8063

References

Battaglia M C *et al* 2016 Dosimetric response of radiochromic films to protons of low energies in the Bragg peak region *Phys. Rev. Accel. Beams* **19** 1–7

Bekerat H *et al* 2014 Improving the energy response of external beam therapy (EBT) GafChromic™ dosimetry films at low energies (⩽100 keV) *Med. Phys.* **41** 022101

Bird R P, Rohrig N, Colvett R D, Geard C R and Marino S A 1980 Inactivation of synchronized Chinese Hamster V79 cells with charged-particle track segments *Radiat.R es.* **82** 277–89

Candler C 1960 The photographic process as a diatomic reaction *Aust. J. Phys.* **13** 419

Candler C 1962 Photographic characteristic of a monolayer *J. Opt. Soc. Am.* **52** 300

Castriconi R *et al* 2017 Dose-response of EBT3 radiochromic films to proton and carbon ion clinical beams *Phys. Med. Biol.* **62** 377–93

Colvett R D and Rohrig N 1979 Biophysical studies with spatially correlated ions. 2. Multiple scattering, experimental facility, and dosimetry *Radiat. Res.* **78** 192–209

Das I J 2018 *Radiochromic Film: Role and Applications in Film Dosimetry* ed I J Das (Boca Raton, FL: CRC Press)

Devic S 2011 Radiochromic film dosimetry: past, present, and future *Phys. Med.* **27** 122–34

Devic S, Tomic N and Lewis D 2016 Reference radiochromic film dosimetry: review of technical aspects *Phys. Med.* **32** 541–56

Fiorini F *et al* 2014 Under-response correction for EBT3 films in the presence of proton spread out Bragg peaks *Phys. Med.* **30** 454–61

Hitchcock F L and Robinson C S 1923 *Differential Equations in Applied Chemistry* (New York: Wiley)

Iqbal K, Mazhar Iqbal M, Akram M, Altaf S and Ahmad Buzdar S 2018 Dosimetric verification and quality assurance for intensity-modulated radiation therapy using Gafchromic® EBT3 film *J. Radiother. Pract.* **17** 85–95

Ju S G *et al* 2010 Comparison of film dosimetry techniques used for quality assurance of intensity modulated radiation therapy *Med. Phys.* **37** 2925–33

Kirby D, Green S, Palmans H, Hugtenburg R, Wojnecki C and Parker D 2010 LET dependence of GafChromic films and an ion chamber in low-energy proton dosimetry *Phys. Med. Biol.* **55** 417–33

Krzempek D *et al* 2018 Calibration of Gafchromic Ebt3 film for dosimetry of scanning proton pencil beam (Pbs) *Radiat. Prot. Dosim.* **180** 324–8

León Marroquin E Y, Herrera González J A, Camacho López M A, Villarreal Barajas J E and García-Garduño O A 2016 Evaluation of the uncertainty in an EBT3 film dosimetry system utilizing net optical density *J. Appl. Clin. Med. Phys.* **17** 466–81

Lewis D and Chan M F 2014 Correcting lateral response artifacts from flatbed scanners for radiochromic film dosimetry *Med. Phys.* **42** 416–29

Marino S A 2017 50 years of the radiological research accelerator facility (RARAF) *Radiat. Res.* **187** 413–23

Martišíková M and Jäkel O 2010 Dosimetric properties of Gafchromic® EBT films in monoenergetic medical ion beams *Phys. Med. Biol.* **55** 3741–51

Massillon-JL G, Chiu-Tsao S-T, Domingo-Muñoz I and Chan M F 2012 Energy dependence of the new Gafchromic EBT3 film: dose response curves for 50 KV, 6 and 15 MV x-ray beams *Int. J. Med. Phys. Clin. Eng. Radiat. Oncol.* **01** 60–5

Mirza J A, Park H, Park S-Y and Ye S-J 2016 Use of radiochromic film as a high-spatial resolution dosimeter by Raman spectroscopy *Med. Phys.* **43** 4520–8

Palmer A L, Nisbet A and Bradley D 2013 Verification of high dose rate brachytherapy dose distributions with EBT3 Gafchromic film quality control techniques *Phys. Med. Biol.* **58** 497–511

Perles L A, Mirkovic D, Anand A, Titt U and Mohan R 2013 LET dependence of the response of EBT2 films in proton dosimetry modeled as a bimolecular chemical reaction *Phys. Med. Biol.* **58** 8477–91

Reinhardt S *et al* 2015 Investigation of EBT2 and EBT3 films for proton dosimetry in the 4–20 MeV energy range *Radiat. Environ. Biophys.* **54** 71–9

Schoenfeld A A, Poppinga D, Harder D, Doerner K-J and Poppe B 2014 The artefacts of radiochromic film dosimetry with flatbed scanners and their causation by light scattering from radiation-induced polymers *Phys. Med. Biol.* **59** 3575–97

Sipilä P, Ojala J, Kaijaluoto S, Jokelainen I and Kosunen A 2016 Gafchromic EBT3 film dosimetry in electron beams—energy dependence and improved film read-out *J. Appl. Clin. Med. Phys.* **17** 360–73

Steenbeke F *et al* 2016 Quality assurance of a 50 kV radiotherapy unit using EBT3 GafChromic film *Technol. Cancer Res. Treat.* **15** 163–70

Vadrucci M *et al* 2015 Calibration of GafChromic EBT3 for absorbed dose measurements in 5 MeV proton beam and ^{60}Co γ-rays *Med. Phys.* **42** 4678–84

Welch D, Randers-Pehrson G, Spotnitz H M and Brenner D J 2017 Unlaminated Gafchromic EBT3 film for ultraviolet radiation monitoring *Radiat. Prot. Dosim.* **176** 341–6

Wen N *et al* 2016 Precise film dosimetry for stereotactic radiosurgery and stereotactic body radiotherapy quality assurance using Gafchromic™ EBT3 films *Radiat. Oncol.* **11** 132

Ziegler J F, Biersack J P and Ziegler M D 2008 *SRIM, The Stopping and Range of Ions in Matter* (Chester, Maryland: SRIM Co) (http://cds.cern.ch/record/1525729) (Accessed: 17 June 2018)